

# Asynchronous Compressive Radar

Jun Zhou<sup>1</sup>, Samuel Palermo<sup>1</sup>, José S. Martínez<sup>1</sup>, Brian M. Sadler<sup>2</sup>, and Sebastian Hoyos<sup>1</sup>

<sup>1</sup>Texas A&M University, College Station, Texas, USA, 77843

<sup>2</sup>US Army Research Laboratory, Adelphi, Maryland, USA, 20783

**Abstract:** A low-power asynchronous compressive sensing scheme is proposed for radar. Power and design cost are optimized by combining asynchronous sampling and compressive sensing which decreases both the duty cycle of front-end circuits and the data volume of the ADC interface. In the signal reconstruction stage, a low-complexity noise-robust split-projection least squares (SPLS) is proposed.

**Keywords:** asynchronous sampling; compressive sensing; continuous-time ternary encoding; split projection.

## Introduction

Radar systems using active arrays are well documented, with several successful implementations [1] and target parameter estimation techniques (size, location, and speed). Beamforming is typically utilized both at the transmitter, where multiple elements that comprise a phase-array steer the energy in a desired direction, and at the receiver as well, where a phase-array implements digital beamforming to select one or several angle of arrivals. This approach enhances the signal energy to noise ratio (SNR) and allows for space-time adaptive processing. Fig. 1 shows radar system in a vehicle-to-vehicle communication and collision avoidance application where low-power miniaturized design and real-time high-resolution target detection are required.

In order to exploit the benefits of digital beamforming at the receiver side, such as low-cost and ease of implementation, high-quality analog-to-digital conversion (ADC) is compulsory in a radar system. Given that a high-resolution radar requires broadband transmitting signals, and that the Nyquist/Shannon theorem necessitates a sampling rate of at least twice the signal bandwidth to avoid image aliasing, an excessive data exists at ADC interface in conventional Nyquist-sampling based architectures. While synthetic impulse and aperture radar (SIAR) may relax the sampling rate for each individual antenna, the aggregated data traffic of multiple orthogonal waveforms remains large. In the near future, the total data volume in high-resolution radar will rapidly grow due to the increasing demand for large active arrays that require a large number of parallel channels. This extremely high data traffic at the ADC not only presents challenges associated with the integration of a massive number of high-speed, high-performance, and low-power ADCs, but also in the high-speed data links between the analog front-end and digital processing unit.

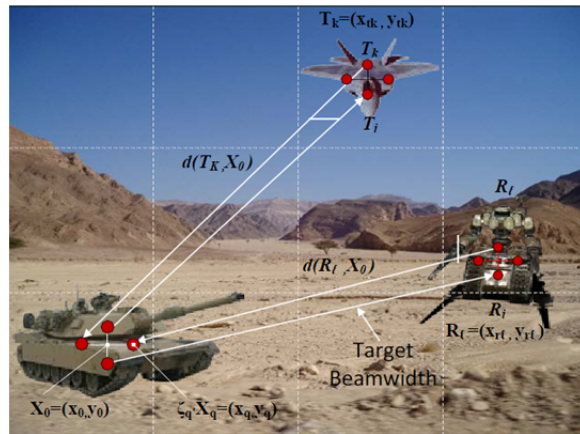


**Figure 1:** Radar system in a vehicle-to-vehicle communication and collision avoidance application.

Advanced signal processing algorithms have been proposed to reduce the data volume in ADC [2]. Nevertheless, they are still confined to Nyquist sampling, stressing the power consumption and cost of analog-to-digital conversion. Now the question is, if the radar signal is compressible, can we achieve the compression at the analog front-end without compromising the signal quality? Recent breakthroughs in compressive sensing (CS) gives an affirmative answer as any sparse signal can be perfectly reconstructed with an overwhelming probability from a much smaller number of incoherent, randomized linear projection samples relative to Nyquist sampling systems [3].

Some radar systems with CS are reported [4], [5] for data compression. An employed random demodulator front-end, which consisting of a dedicated mixer and an integrator, implements CS front-end in [4]. In this architecture the mixer must operate at or above the Nyquist rate for incoherent sampling, resulting in significant dynamic power; and the integrator also produces considerable static power during the charge accumulation stage. As both the mixer and integrator are active throughout measurement generation, the random demodulator approach consumes an excessive amount of power. In addition, the dedicated analog circuitry must display high linearity, as non-linear distortion is difficult to remove in the sparse recovery stage and will affect the reconstruction performance [6]. An alternative modulated-wave converter approach [5] also achieve sub-Nyquist sampling at expense of an active channel count of no fewer than four times the band number, resulting in increased overhead. Besides, challenges are faced in the  $T$ -periodic waveforms generation hardware.

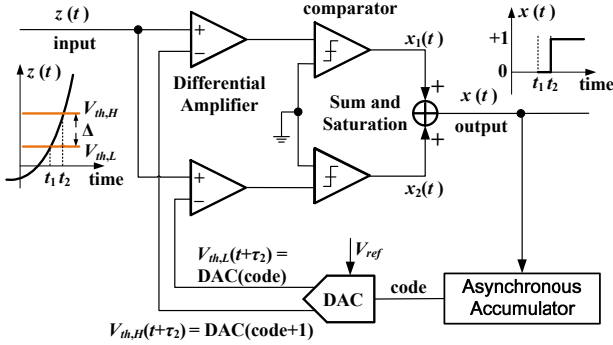


Figure 2: Block diagram of the CT-TE scheme.

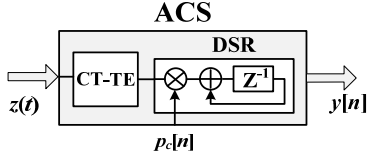


Figure 3: Block diagram of the asynchronous compressive sensing architecture.

In this paper, we present a novel low-power asynchronous compressive sensing (ACS) scheme for high-resolution radar. The embedded CS technique allows compressed data volume at the ADC interface, which facilitates massive integration in large active array radars and relaxes the high-speed data links' requirements. The asynchronous sampling improves the energy efficiency by decreasing duty cycle of power-demanding circuits. Specifically, we present a continuous-time ternary encoding (CT-TE) scheme to convert signal variations to ternary timing information [7]. A digital random sampler (DRS) is designed to sample the ternary timing signal at sub-Nyquist rate, which shows low power, ease of integration and excellent linearity in the compressed sampling. We also propose a novel low-cost and noise-robust signal reconstruction algorithm for ACS front-end, called split-projection least squares (SPLS). The SPLS scheme is the first to translate the complicated nonlinear sparse reconstruction problem into a series of independent  $l_2$ -norm problems that can be efficiently implemented by standard least squares (LS) estimator. It decreases the computation cost in signal reconstruction and potentially supports real-time processing of radar signals.

### Asynchronous Compressive Sensing Front-end

Compressive Sensing (CS) is a framework that enables sub-Nyquist sampling and processing of sparse signals. A sufficiently sparse or compressible signal can be reliably reconstructed from a relatively small number of incoherent, randomized linear projection samples as compared to the conventional Nyquist sampling systems [3]. One unique advantage of the CS technique is that it integrates sampling and compression into one step at the analog front-end.

CS adopts a randomized sampling kernel rather than the conventional delta streams. At the signal recovery stage, CS reconstructs the original signal by solving an optimization problem,

$$\min \|x\|_1 \quad \text{subject to} \quad y = \Phi x, \quad (1)$$

where  $\Phi$  is an  $M \times N$  measurement matrix. As is well known [3], problem (1) is equivalent to an  $l_0$ -norm problem when  $\Phi$  satisfies a restricted isometry property (RIP). Composing  $\Phi$  from Gaussian and/or symmetric Bernoulli ( $\pm 1$ ) random processes satisfies RIP with overwhelming probability [3].

Fig. 2 shows the block diagram of the CT-TE scheme where a  $Q$ -bits DAC divides the signal swing  $U$  equally into  $2^Q$  levels. At any instant, the DAC provides a pair of thresholds ( $V_{th,L}$ ,  $V_{th,H}$ ) to the comparator, which virtually forms a comparison window. When input  $z(t)$  goes higher than  $V_{th,H}$  or lower than  $V_{th,L}$ , the comparator outputs ternary state "1" or "-1", respectively; otherwise, the comparator outputs "0". The following asynchronous adder and accumulator are level-sensitive combinational logic, which record signal variations and update the DAC input accordingly. By this way, amplitude variations in  $z(t)$  are modulated to ternary timing signal  $x(t)$ . Hence, the CT-TE scheme operates in an asynchronous mode and exhibits excellent power efficiency in capturing impulse-radio types of radar transmit signals.

The CT-TE output is captured by the DRS. Due to ternary state of  $x(t)$ , a simplified DRS with only one adder and one accumulator is used for the sub-Nyquist rate sampling. The inner product calculation in CS scheme is implemented by a digital switch and an accumulator. Digital circuits also offer scaling advantages in advanced technology nodes.

### Split-Projection Least Squares

In this section, we propose a low-complexity signal recovery algorithm to reconstruct the ternary timing signals from the compressed samples generated by the ACS front-end.

Let  $x \in \mathbb{R}^N$  for the  $K$ -sparse signal, and  $y \in \mathbb{R}^M$  for the CS measurements  $y = \Phi x + w$ , where  $\Phi = [\varphi_1, \varphi_2, \varphi_3, \dots, \varphi_N]$ ,  $\varphi_i$  denotes the  $i^{\text{th}}$  column of  $\Phi$ , and  $w$  is Gaussian white noise with zero mean, i.e.,  $w \sim \mathcal{N}(0, \sigma^2)$ .

Define a window  $\Omega$  of length  $L$  to sweep along the columns of  $\Phi$ . At each time, a portion of the columns is selected. Then,  $\Phi$  is split into  $(N/L)$  mutually exclusive sub-matrices,

$$\Phi = \left( \Phi^{(1)}, \Phi^{(2)}, \dots, \Phi^{(N/L)} \right). \quad (2)$$

For the  $i^{\text{th}}$  sub-matrix in (2),  $\Phi$  can be represented by two  $M \times N$  matrices  $\Phi_{\Omega}^{(i)}$  and  $\Phi_{\bar{\Omega}}^{(i)}$  according to the specific  $\Omega = \{S, S+1, \dots, S+L-1\}$ , where  $S \in [1, N-L+1]$ . Dropping the index  $i^{\text{th}}$  for convenience,

$$\Phi = \Phi_{\Omega} + \Phi_{\bar{\Omega}}, \quad (3)$$

$$\Phi_{\Omega} = \begin{pmatrix} \mathbf{0}_{M \times (S-1)} & [\mathbf{B}_2]_{M \times L} & \mathbf{0}_{M \times (N-S-L+1)} \end{pmatrix}, \quad (4)$$

$$\Phi_{\tilde{\Omega}} = \begin{pmatrix} [\mathbf{B}_1]_{M \times (S-1)} & \mathbf{0}_{M \times L} & [\mathbf{B}_3]_{M \times (N-S-L+1)} \end{pmatrix}, \quad (5)$$

where sub-matrices  $\mathbf{B}_1$ ,  $\mathbf{B}_2$ , and  $\mathbf{B}_3$  are formed by columns of  $\Phi$  parameterized by  $\Omega$ . Similarly, we can also segment  $x$  based on  $\Omega$ ,

$$x = \begin{pmatrix} [x_1^T]_{1 \times (S-1)} & [x_2^T]_{1 \times L} & [x_3^T]_{1 \times (N-S-L+1)} \end{pmatrix}^T. \quad (6)$$

Combining Eqs. (3)-(6), the compressed measurement can be rewritten as follows,

$$y = \mathbf{B}_2 x_2 + (\mathbf{B}_1 x_1 + \mathbf{B}_3 x_3) + w. \quad (7)$$

Targeting an unknown  $x_2$ , the log-likelihood function is,

$$\begin{aligned} \ln \Pr(y; x_2) &= -\frac{1}{2} \ln(2\pi\sigma^2) \\ &- \frac{1}{2\sigma^2} (y - \mathbf{B}_2 x_2 - \mathbf{B}_1 x_1 - \mathbf{B}_3 x_3)^T (y - \mathbf{B}_2 x_2 - \mathbf{B}_1 x_1 - \mathbf{B}_3 x_3) \end{aligned} \quad (8)$$

Here,  $\Phi$  has full column rank due to the RIP constraint. Hence,  $\mathbf{B}_2^T \mathbf{B}_2$  is invertible if  $L \leq M$ . The first derivative of the log-likelihood function with respect to  $x_2$  is

$$\frac{\partial \ln \Pr(y; x_2)}{\partial x_2} = \frac{\mathbf{B}_2^T \mathbf{B}_2}{\sigma^2} \cdot \left\{ (\mathbf{B}_2^T \mathbf{B}_2)^{-1} \mathbf{B}_2^T y - \tilde{x}_2 \right\}, \quad (9)$$

where  $\tilde{x}_2 = x_2 + (\mathbf{B}_2^T \mathbf{B}_2)^{-1} \mathbf{B}_2^T (\mathbf{B}_1 x_1 + \mathbf{B}_3 x_3)$  is the expectation of the estimator  $\hat{x}_2 = (\mathbf{B}_2^T \mathbf{B}_2)^{-1} \mathbf{B}_2^T y$ . The SPLS reconstructs the entire signal by sweeping all the columns and stacking each window-based estimate along the signal's dimension. If  $\mathbf{B}_2^T \mathbf{B}_1$  and  $\mathbf{B}_2^T \mathbf{B}_3$  are 0, or  $x_1$  and  $x_3$  are 0, the proposed SPLS estimator is interference-free and becomes Minimum-Variance Unbiased (MUV) estimator, which has expectation equal to the true value, and the variance achieves the Cramér–Rao Lower Bound (CRLB).

$$\text{CRLB}(\hat{x}_2) = (I_{x_2})^{-1}, \quad \text{where } I_{x_2} = \sigma^2 (\mathbf{B}_2^T \mathbf{B}_2)^{-1}. \quad (10)$$

The SPLS estimator can be rewritten as

$$\hat{x}_2 = (\mathbf{B}_2^T \mathbf{B}_2)^{-1} \mathbf{B}_2^T y. \quad (11)$$

Eq. (11) provides an estimate for a section of  $x$ , i.e.,  $x_2$ . The entire estimate is formed by stacking the section estimates along the signal dimension. Note that each section estimate is non-adaptive, and independent of each other, which is fundamentally different from the iteratively reweighted least squares (IRLS) algorithm [8]. These unique advantages potentially support a fully parallel hardware for real-time signal reconstruction. The pseudo-code for the SPLS scheme is shown in **Algorithm 1**.

---

#### Algorithm 1: Split-Projection Least Squares (SPLS)

---

INPUT: sensing matrix  $\Phi$ , compressed signal  $y$ , the length of window  $L$ , and the dimension of input sparse signal  $N$ .

OUTPUT: the estimate of input sparse signal  $\hat{x}$

---

PROCEDURE:

1. Initialize the first split by setting  $S = 1$ . The column indexes in the window is  $\Omega = \{S, S + 1, \dots, S + L -$
- 

TABLE I  
RADAR SYSTEM SPECIFICATIONS

Parameter	Value
MAX Unambiguous Range	90 meter
Range Resolution	0.02 meter
Transmit Pulse	LFM: 8GHz bandwidth 1.25ns pulse width
Peak Transmit Power	70mW
Target Type	Swerling-2 type

1}, and initialize the estimate of input signal  $\hat{x} = \emptyset$ .

2. **while**  $S < N$
  3. Draw sub-matrix  $\mathbf{B}_2$  from  $\Phi$  according to  $\Omega$ .
  4. Obtain the SPLS estimate,  $\hat{x}_2 = (\mathbf{B}_2^T \mathbf{B}_2)^{-1} \mathbf{B}_2^T y$ .
  5. Stack the section estimate,  $\hat{x} = [\hat{x}; \hat{x}_2]$ .
  6. Update the starting point of window,  $S = S + L$ .
  7. **end while and return**  $\hat{x}$
- 

Amplitude detection is performed on estimate  $\hat{x}$  to exploit the ternary structure, i.e., because  $x \in \{-1, 0, 1\}$ . We derive an appropriate threshold in the following. With Gaussian noise,  $p$  estimates of  $x$ ,  $(x)_1, (x)_2, (x)_3, \dots, (x)_p$ , are normal with mean  $\bar{x}_p$ , and standard deviation  $\text{Std}(x_p)$ . The resulting  $t$ -value is [9],

$$t = \frac{\bar{x}_p - x}{\text{Std}(x_p) / \sqrt{p}}. \quad (12)$$

The new test statistic  $t$  follows a  $(p-1)$  degree of freedom Student's  $t$ -distribution. A number  $T_\alpha$  is chosen to have a  $100(1-\alpha)\%$  confidence interval, i.e.  $\Pr(-T_\alpha < t < T_\alpha) = 1 - \alpha$ ,

$$\Pr\left(\bar{x}_p - T_\alpha \cdot \frac{\text{Std}(x_p)}{\sqrt{p}} < x < \bar{x}_p + T_\alpha \cdot \frac{\text{Std}(x_p)}{\sqrt{p}}\right) = 1 - \alpha. \quad (13)$$

Therefore, the endpoints of this confidence interval and the optimal thresholds  $TH$  for hypothesis testing are

$$TH = \bar{x}_p \pm T_\alpha \cdot \frac{\text{Std}(x_p)}{\sqrt{p}}. \quad (14)$$

## Simulations

A vehicle-to-vehicle monocratic pulsed radar is constructed based on the key parameters listed in Table I. Three stationary Swerling case 2 targets are simulated, located at 3.925m, 8.155m and 19.844m. Targets have  $1\text{m}^2$  radar cross section.

We employ the ACS scheme as the CS front-end to test the feasibility and performance of signal recovery via the SPLS. Various signal recovery methods in CS area are compared, including Basis Pursuit [10], Orthogonal Matching Pursuit (OMP) [11], stage-wise Orthogonal Matching Pursuit (StOMP) [12], Bayesian Compressive Sensing (Bayesian CS) [13], and Smoothed-L0 [14].

As a preliminary test, the ternary timing signals generated by the 4-bit CT-TE scheme is compressed sampled by the DRS module. The ternary timing signals have a dimension

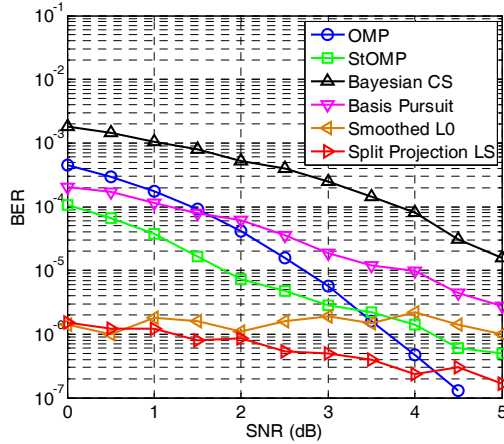


**Figure 4:** BER of recovered signal after amplitude detection at a normalized SSR of 6%. 10,000 independent simulations of ternary sparse signal with dimension 10,000.

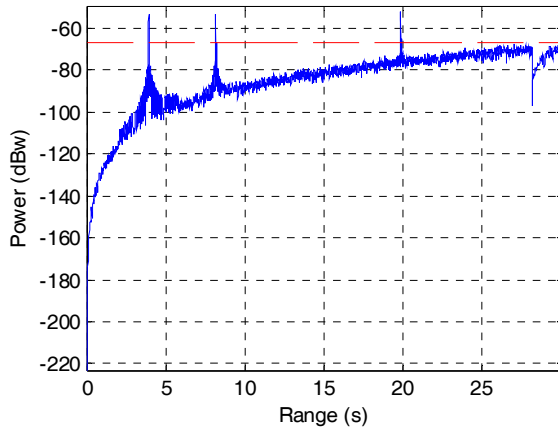


**Figure 5:** Target detection in the proposed compressed radar system with the ACS front-end.

of 10,000, and an averaged sparsity of 0.12%. For low signal-to-noise ratio (SNR) in radar applications, we simulate an SNR from 0dB to 5dB when  $M = 600$ , i.e. a normalized sub-Nyquist sampling ratio (SSR) of 6%. SNR is defined as the power ratio between signal and observation noise,

$$SNR = \frac{P_{\text{signal}}}{P_{\text{noise}}} \quad (15)$$

10,000 independent simulations are carried out for Monte-Carlo simulation. Fig. 4 shows the bit error rate (BER) performance after amplitude detection. For the conventional signal recovery algorithms, the threshold is set to 0.5 due to their unbiased estimation. While the SPSL estimator has thresholds determined by (14). Fig. 4 demonstrates the SPSL scheme has the best BER after amplitude detection among all the other signal recovery schemes in low SNR region.

Fig. 5 shows the target detection in the proposed compressed radar system. The solid line is the reconstructed pulse signal. The dashed line is the power threshold for detection using Shnidman's equation. As shown, three targets are detected at

3.928m, 8.156m, and 19.847m, respectively, satisfying the range resolution requirement.

## Conclusion

In this paper, we present an asynchronous compressed radar system with the ACS front-end. For the signal recovery stage, a low-complexity noise-robust SPSL is proposed.

## References

1. J. A. Malas, "F-22 radar development," in *Proc. of IEEE National conf. on Aerospace and Electronics*, pp. 831 – 839, 1997.
2. Y. Huang and W. Ai, "Weather radar data compression based on zerotree wavelet algorithm," *IEEE Int'l Image and Signal Proc.*, 2009.
3. E. J. Candès, M. B. Wakin, "An Introduction to Compressive Sampling," *IEEE Signal Proc. Magazine*, vol. 25, no. 2, 2008.
4. M.A. Herman and T. Strohmer, "High-resolution radar via compressed sensing," *IEEE Trans. on Signal Proc.*, vol. 57, no. 6, 2009.
5. M. Mishali and Y. C. Eldar, "From theory to practice: Sub-Nyquist sampling of sparse wideband analog signals," *IEEE J. Sel. Topics Signal Process.*, vol. 4, no. 2, pp. 375-391, Apr. 2010.
6. Z. Yu, J. Zhou, M. Ramirez, S. Hoyos, B.M. Sadler, "The Impact of ADC Nonlinearity in a Compressive Sensing Receiver for Frequency-Domain Sparse Signals," *J. of Phy. Comm.*, vol. 5, no. 2, 2012.
7. J. Zhou, M. Ramirez, S. Palermo, S. Hoyos, "Digital-Assisted Asynchronous Compressive Sensing Front-end," *IEEE J. on Emerging and Selected Topics in Circuits and Systems*, vol.2, no.3, pp.482 – 492, 2012.
8. B. Wohlberg and P. Rodriguez, "An iteratively reweighted norm algorithm for minimization of total variation functionals," *IEEE Signal Processing Letters*, vol. 14, no. 12, pp. 948-951, Dec. 2007.
9. R. E. Walpole, R. H. Myers, S. L. Myers, "Probability and Statistics for Engineers and Scientists," Pearson Education, 7th edition, pg. 237, ISBN 81-7758-404-9.
10. E. Candès, J. Romberg and T. Tao, "Robust uncertainty principles: Exact signal reconstruction from highly incomplete frequency information," *IEEE Trans. Inform. Theory*, vol.52, no.2, pp.489–509,2006.
11. J. A. Tropp and A. C. Gilbert, "Signal Recovery from Random Measurements via Orthogonal Matching Pursuit," *IEEE Trans. Inform. Theory*, vol. 53, no. 12, pp. 4655–4666, Dec. 2007.
12. D. Donoho, Y. Tsaig, I. Drori, and J. Starck, "Sparse solution for underdetermined linear equations by stagewise orthogonal matching pursuit," *IEEE Trans. on Inform. Theory*, vol. 58, no. 2, pp.1094–1121, 2012.
13. S. Ji, Y. Xue, and L. Carin, "Bayesian Compressive Sensing," *IEEE Trans. Inform. Theory*, vol. 56, no. 6, pp. 2346–2356, Jun. 2008.
14. G. H. Mohimani, M. B. Zadeh, and C. Jutten, "Complex-valued sparse representation based on smoothed l0 norm," in *Proc. of IEEE Int. Conf. on Acoustics, Speech, and Signal Processing* pp. 3881–3884, Apr. 2008.